
Prompt Ensemble Self-training for Open-Vocabulary Domain Adaptation

Jiaxing Huang*, Jingyi Zhang*, Han Qiu, Sheng Jin, Shijian Lu[†]

S-lab, School of Computer Science and Engineering, Nanyang Technological University

{Jiaxing.Huang, Jingyi.Zhang, Sheng.Jin, Shijian.Lu}@ntu.edu.sg

han023@e.ntu.edu.sg

Abstract

Traditional domain adaptation assumes the same vocabulary across source and target domains, which often struggles with limited transfer flexibility and efficiency while handling target domains with different vocabularies. Inspired by recent vision-language models (VLMs) that enable open-vocabulary visual recognition by reasoning on both images and texts, we study open-vocabulary domain adaptation (OVDA), a new unsupervised domain adaptation framework that positions a pre-trained VLM as the source model and transfers it towards arbitrary unlabelled target domains. To this end, we design a Prompt Ensemble Self-training (PEST) technique that exploits the synergy between vision and language to mitigate the domain discrepancies in image and text distributions simultaneously. Specifically, PEST makes use of the complementary property of multiple prompts within and across vision and language modalities, which enables joint exploitation of vision and language information and effective learning of image-text correspondences in the unlabelled target domains. Additionally, PEST captures temporal information via temporal prompt ensemble which helps memorize previously learnt target information. Extensive experiments show that PEST outperforms the state-of-the-art consistently across 10 image recognition tasks.

1 Introduction

Deep learning-based vision models [17, 8] have achieved great success in myriad image recognition tasks but at the price of laborious annotation of large-scale training images [7]. To circumvent the annotation constraint, domain adaptation (DA) [33, 24] has been explored to transfer a vision model pre-trained in certain labelled source domains towards unlabelled target domains by mitigating the inter-domain discrepancies in image distributions. However, traditional DA [56, 33, 24] assumes that source and target domains have the same vocabulary. It struggles while handling target domains with different vocabularies, limiting its flexibility and efficiency greatly in unsupervised transfer.

Inspired by recent vision-language models (VLMs) [42] that enable open-vocabulary visual recognition by reasoning on both images and texts, we study open-vocabulary domain adaptation (OVDA), a new unsupervised domain adaptation (UDA) framework that positions a pre-trained VLM as the source model and transfers it towards arbitrary unlabelled target domains. OVDA requires a single pre-trained VLM only while transferring towards target domains of different vocabularies, instead of preparing multiple vocabulary-specific vision models with respective source datasets, as illustrated in Fig. 1. In addition, OVDA allows unsupervised transfer towards new domains with customized vocabulary, which greatly mitigates the image annotation constraint and facilitates deep network training while handling various new visual recognition tasks. On the other hand, the shift from

*indicates equal contribution.

[†]corresponding author.

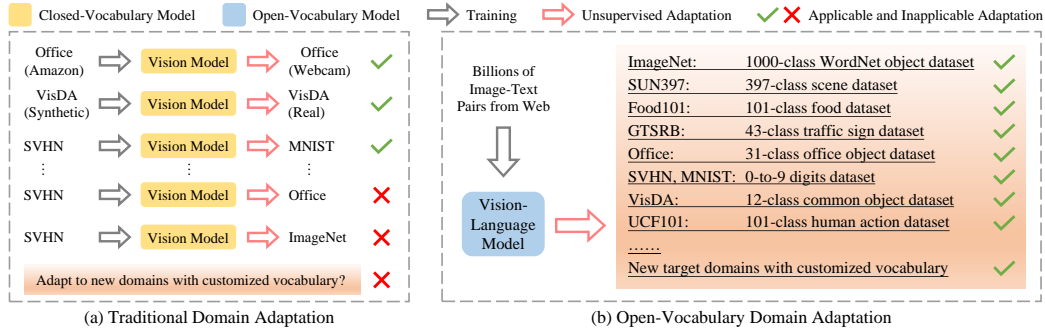


Figure 1: Traditional domain adaptation transfers a vision model across domains of the same vocabulary, which struggles while handling target domains with different vocabularies or new domains with customized vocabularies as illustrated in (a). Inspired by the recent open-vocabulary vision-language models (VLMs), we study open-vocabulary domain adaptation, a new unsupervised domain adaptation framework that positions a single pre-trained VLM as the source model and transfers it towards arbitrary unlabelled target domains as illustrated in (b).

traditional domain adaptation toward OVDA comes with a new challenge, namely, the cross-domain discrepancies in both image distributions and text distributions.

Drawing inspiration from the recent advances in multi-prompt learning [28, 49, 41, 66] in natural language processing (NLP), we design PEST, a Prompt Ensemble Self-training technique that exploits the synergy between vision and language to mitigate the domain discrepancies in image and text distributions simultaneously while self-training. PEST makes use of the complementary property of multiple prompts within and across vision and language modalities: it exploits VLMs to encode the image prompts [38, 67] and text prompts [38, 67] into an aligned vision-language feature space and fuses the encoded visual and textual features to “prompt” unsupervised self-training for more accurate pseudo label prediction. This enables joint exploitation of vision and language information and effective learning of image-text correspondences in the unlabelled target domains. In addition, PEST captures temporal information via temporal prompt ensemble, which helps memorize previously learnt target information by fusing the prompts encoded by the intermediate models evolved along the adaptation process.

The proposed PEST can be viewed as a new type of self-training with multi-prompt learning for the task of OVDA. It has three desirable advantages: 1) it introduces vision prompt ensemble and language prompt ensemble and enables simultaneous mitigation of image and text discrepancies across domains effectively; 2) it introduces temporal prompt ensemble along the adaptation process which allows harvesting previously learnt target information effectively; 3) it works within an aligned image-text feature space which allows prompt ensemble not only within but also across vision, language and temporal dimensions, capturing their complementary advantages effectively.

In summary, the contributions of this work are threefold. *First*, we design a novel open-vocabulary domain adaptation framework that explores multi-prompt learning upon self-training to learn effective image-text correspondences over unlabelled target images. To the best of our knowledge, this is the first work that explores multi-prompt learning for OVDA. *Second*, we design prompt ensemble self-training that introduces prompt ensemble over vision, language and temporal dimensions for simultaneous mitigation of image and text discrepancies in OVDA. *Third*, extensive experiments show that the proposed prompt ensemble self-training outperforms the state-of-the-art consistently across multiple image recognition tasks.

2 Related Work

Domain Adaptation (DA), a type of unsupervised transfer learning, aims to adapt a model pre-trained on certain labelled source domains towards unlabelled target domains. Most existing DA methods can be broadly grouped into two categories. The first category employs *adversarial learning* to align source and target image distributions over the input space [18, 23, 25, 69, 48, 32, 19, 63], feature space [56, 53, 20, 70, 60, 11], output space [45, 12, 39, 46] or latent space [58, 26, 54, 3, 71], for mitigating the distribution discrepancy across domains. The second approach explores *self-training*

that learns from unlabelled target images with predicted pseudo labels [76, 24, 47, 72, 21, 77, 22, 10, 33, 34]. Despite their great success, most existing methods assume the same vocabulary across the source and target domains and cannot handle target domains with different vocabulary or new domains with customized vocabulary. This limits the flexibility and efficiency of DA greatly. We study open-vocabulary domain adaptation in this work, a new framework that reasons both images and texts and allows unsupervised transfer learning towards arbitrary unlabelled target domains. We design prompt ensemble self-training that explores the synergy of vision and language to mitigate image and text domain gaps simultaneously in OVDA.

Vision Language Model (VLM) [42, 27, 65, 64, 55, 68] aims to learn effective vision-language correlation from image-text pairs that are almost infinitely available on the Web. It has demonstrated great potential in open-vocabulary visual recognition by recognizing images with arbitrary texts. As a representative, CLIP [42] collects 400 million image-text pairs from the Web and learns rich vision-language correlation via image-text contrastive learning. Despite its great success, VLMs often suffer from degraded performance due to cross-domain discrepancies with respect to various downstream domains. Unlike recent attempts [74, 73] that adapt VLMs with few-shot labelled target images, we focus on adapting VLMs towards various downstream domains by ingeniously exploiting the unlabelled target images which are often off-the-shelf available in abundance.

Multi-Prompt Learning explores complementary advantages of different prompts [28] which was originally designed for effective transfer of large language models in NLP. Most existing methods can be broadly grouped into three categories. The first is *prompt ensembling* that creates multiple unanswered prompts for an input to predict via uniform averaging [28, 49, 66], weighted averaging [28, 41, 49], majority voting [30, 14], etc. The second exploits *prompt augmentation* that provides several answered prompts for an input for better predictions, where most studies focus on the selection [9, 37, 35] and ordering [37, 29, 13] of answered prompts. The third works by *prompt composition or decomposition* [15, 6], which constructs multiple sub-prompts for better predictions.

3 Method

3.1 Preliminaries of Vision-Language Model

Vision-language model (VLM) training. VLM [42, 27, 65, 64, 55] learns effective vision-language correlation from image-text pairs that are almost infinitely available on the Web [42, 50]. The training involves a VLM $F = \{F^I, F^T\}$ where F^I and F^T denote an image encoder and a text encoder respectively, and an image-text dataset $D_s = \{(x_n^I, x_n^T)\}_{n=1}^N$ where x_n^I and x_n^T stand for an image sample and its paired text sample. Given F and D_s , rich vision-language correlation can be learnt with a vision-language training objective such as image-text contrast [42] as follows:

$$\mathcal{L}_{\text{VLM}} = - \sum_{i=1}^N \log \frac{\exp(z_i^I \cdot z_i^T / \tau)}{\sum_{j=1}^N \exp(z_i^I \cdot z_j^T / \tau)} - \sum_{i=1}^N \log \frac{\exp(z_i^T \cdot z_i^I / \tau)}{\sum_{j=1}^N \exp(z_i^T \cdot z_j^I / \tau)}, \quad (1)$$

where the two terms on the right denote image-to-text and text-to-image contrastive losses respectively. The notations $z_i^I = F^I(x_i^I)$ and $z_i^T = F^T(x_i^T)$ stand for the encoded image and text features respectively, τ denotes a temperature parameter [61], and “ \cdot ” stands for the inner-product that measures the cosine similarity between two features.

VLM inference. A pre-trained VLM can perform open-vocabulary image recognition on arbitrary unlabelled target domains by reasoning on both images and texts [42]. Given an arbitrary unlabelled target dataset $D = \{X^I, X^T\}$, $X^I = \{x_n^I\}_{n=1}^N$ stands for N unlabelled images and $X^T = \{x_m^T\}_{m=1}^M$ denotes M class names of interest, e.g., $X^T = \{\text{car, bus, ..., bike, person}\}$. The pre-trained VLM predicts the probability of an image x^I belonging to class x^T by:

$$p_{x^I \rightarrow x^T} = z^I \cdot z^T, \quad (2)$$

where $z^I = F^I(x^I)$, $z^T = F^T(x^T)$. Theoretically, VLMs can work with any class names X^T and thus achieve open-vocabulary image recognition. Note $X^T = \{x_m^T\}_{m=1}^M$ contains M target-domain class names but provides no information of which image belongs to which class name [42].

On the other hand, the performance of VLM is often constrained on target data [74, 31] due to cross-domain discrepancies in both image distributions and text distributions.

3.2 Definition of Open-vocabulary Domain Adaptation (OVDA)

This work focuses on the task of OVDA, a new unsupervised domain adaptation (UDA) framework that transfers a pre-trained VLM $F = \{F^I, F^T\}$ towards an arbitrary unlabelled target domain $D = \{X^I, X^T\}$ with certain unsupervised training losses, i.e., $\mathcal{L}_{\text{OVDA}} = \mathcal{L}_{\text{unsupervised}}(X^I, X^T; F^I, F^T)$. Take self-training [75, 76] as an example. Given $X^I = \{x_n^I\}_{n=1}^N$ and $X^T = \{x_m^T\}_{m=1}^M$, the unsupervised training loss on unlabelled target data can be formulated as the following:

$$y_n^I = \arg \max_m z_n^I \cdot z_m^T, \quad \mathcal{L}_{\text{ST}} = - \sum_{n=1}^N \log \frac{\sum_{m=1}^M \exp(z_n^I \cdot z_m^T / \tau) \times \mathbb{1}(\hat{y}_n^I == m)}{\sum_{m=1}^M \exp(z_n^I \cdot z_m^T / \tau)}, \quad (3)$$

where z_n^I and z_m^T denote the encoded image and text features, i.e., $z_n^I = F^I(x_n^I)$ and $z_m^T = F^T(x_m^T)$. y_n^I stands for the pseudo label of x_n^I .

Note the unsupervised training is often unstable and susceptible to collapse if we optimize VLM image encoder and text encoder concurrently [31]. Hence, we freeze the VLM text encoder during unsupervised domain adaptation for stable adaptation.

3.3 Prompt Ensemble Self-training

We tackle the challenge of OVDA from a perspective of multi-prompt learning [28, 49, 66]. As illustrated in Fig. 2, we design prompt ensemble self-training (PEST) that introduces language prompt ensemble and vision prompt ensemble over self-training to mitigate the domain discrepancies in image and text distributions simultaneously. In addition, PEST captures temporal information via temporal prompt ensemble, which helps memorize previously learnt target information by fusing the prompts encoded by the intermediate models evolved along the adaptation process.

Language prompt ensemble fuses the text features generated from different text prompts, aiming to leverage the complementary information of multiple text prompts (i.e., various text descriptions for a class [38, 67]) to mitigate the cross-domain discrepancy in text distributions. It employs a Large Language Model [2, 59] (LLM) to generate multiple text prompts for a given class name and then encodes them by the VLM text encoder. The encoded text features are then fused in a two-step manner: 1) uniformly average the multiple text features to acquire an initial prompt centroid 2) calculate the final prompt centroid by weighted average where the weight of each feature is the distance between it and the initial prompt centroid. This two-step operation allows smooth prompt fusion by weighting down the effect of corner cases, which is important for language prompt ensemble as the LLM-generated prompts are not always reliable (e.g., when experiencing generation failures, LLM may generate only a full stop character “.” or a random word).

Given a class name $x_n^T \in X^T$, we employ the Large Language Model [2] to generate K text prompts $\{x_{(m,1)}^T, x_{(m,2)}^T, \dots, x_{(m,K)}^T\}$ and then the VLM text encoder F^T to encode the generated prompts to acquire text features $\{z_{(m,1)}^T, z_{(m,2)}^T, \dots, z_{(m,K)}^T\}$ (i.e., $z_{(m,k)}^T = F^T(x_{(m,k)}^T)$). The text features are then fused in a two-step manner to get the final text prompt centroid δ_m^T :

$$\delta_m^{T_{\text{initial}}} = \frac{1}{K} \sum_{k=1}^K z_{(m,k)}^T, \quad \delta_m^T = \sum_{k=1}^K (z_{(m,k)}^T \cdot \delta_m^{T_{\text{initial}}}) \times z_{(m,k)}^T, \quad (4)$$

where “ \cdot ” denotes inner-product and $(z_{(m,k)}^T \cdot \delta_m^{T_{\text{initial}}})$ measures the distance between $z_{(m,k)}^T$ and $\delta_m^{T_{\text{initial}}}$.

Vision prompt ensemble fuses the image features generated from multiple image prompts, aiming to utilize the complementary property of multiple image prompts (i.e., various image descriptions for a class [38, 67]) for mitigating the cross-domain discrepancy in image distributions. Given an image, it employs certain off-the-shelf image augmentation policies [5] to generate multiple image prompts, encodes them with the VLM image encoder, and fuses the encoded image features in a class-wise manner. Since target images are unlabelled, we generated pseudo labels for class-wise image feature fusion. The class-wise feature fusion allows category-wise image prompt consolidation, which is crucial to visual prompt ensemble due to the abundance of target images and the encoded image features. In addition, it simplifies vision-language prompt ensembling greatly (described in the later paragraphs) as language prompt ensemble also works in a category-wise manner. Besides,

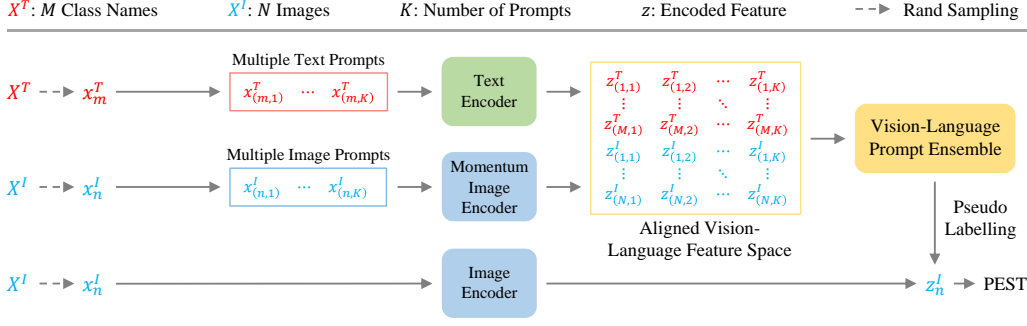


Figure 2: **Overview of Prompt Ensemble Self-training (PEST)**. PEST exploits the complementary property of multiple prompts within and across vision and language modalities, which enables joint exploitation of vision and language information and effective learning of image-text correspondences in the unlabelled target domains. Besides, PEST captures temporal information via temporal prompt ensemble along the training process, which helps memorize previously learnt target information.

with temporal prompt ensembling (described in the later paragraphs), it allows to dynamically select image prompts using pseudo labels along the adaptation process to describe each class visually.

Given an image $x_n^I \in X^I$, we adopt the off-the-shelf image augmentation policies in [5] to generate K image prompts $\{x_{(n,1)}^I, x_{(n,2)}^I, \dots, x_{(n,K)}^I\}$ and then the VLM image encoder F^I to encode the generated image prompts to acquire image features $\{z_{(n,1)}^I, z_{(n,2)}^I, \dots, z_{(n,K)}^I\}$ (i.e., $z_{(n,k)}^I = F^I(x_{(n,k)}^I)$). Finally, the encoded features are fused in a class-wise manner to get the image prompt centroid δ_m^I :

$$\delta_m^I = \frac{1}{\sum_n \sum_{k=1}^K \mathbb{1}(\hat{y}_{(n,k)}^I == m)} \sum_n \sum_{k=1}^K z_{(n,k)}^I \times \mathbb{1}(\hat{y}_{(n,k)}^I == m), \quad (5)$$

where $\mathbb{1}(\hat{y}_{(n,k)}^I == m)$ returns “1” if $\hat{y}_{(n,k)}^I = m$ else 0. Note $\hat{y}_{(n,k)}^I = \arg \max_m z_{(n,k)}^I \cdot z_m^T$ denotes the pseudo label of $x_{(n,k)}^I$. Note we employ the momentum update of F^I in the vision prompt ensemble for stable feature encoding and better capturing of temporal information, as shown in Fig. 2.

Temporal vision-language prompt ensemble exploits the synergy between vision and language by fusing multiple text prompts and multiple image prompts over an aligned vision-language feature space. It employs the text and image prompt centroids as starting point and updates them with the image prompt centroids generated by the intermediate VLM image encoder evolved along the adaptation process. This enables prompt ensemble not only within but also across vision and language modalities, capturing the complementary advantages of vision and language information effectively. In addition, the updating also achieves **temporal prompt ensemble** that captures previously learnt target information effectively. Note we conduct temporal ensemble for image prompts only as the VLM text encoder is frozen during the adaptation process.

Specifically, we use the text and image prompt centroids δ_m^T and δ_m^I to initialize the image-text prompt centroid δ_m^{IT} and keep updating δ_m^{IT} with δ_m^I along the adaptation process as follows:

$$\delta_m^{IT \text{ initial}} = \delta_m^I + \delta_m^T, \quad \delta_m^{IT*} \leftarrow \lambda \delta_m^{IT} + (1 - \lambda) \delta_m^I, \quad (6)$$

where δ_m^{IT} and δ_m^{IT*} denote the image-text prompt centroid before and after one update, respectively. λ is a coefficient that controls the update speed of temporal ensemble. Note the first part denotes *vision-language prompt ensemble* while the second part denotes *temporal prompt ensemble*.

Prompt ensemble self-training. Given image-text prompt centroid δ_m^{IT} , target images, $X^I = \{x_n^I\}_{n=1}^N$ and target class names $X^T = \{x_m^T\}_{m=1}^M$, we employ δ_m^{IT} to “prompt” unsupervised self-training, which can be formulated as follows:

$$y_n^I = \arg \max_m (z_n^I \cdot z_m^T) \times (z_n^I \cdot \delta_m^{IT}), \quad (7)$$

$$\mathcal{L}_{\text{PEST}} = - \sum_{n=1}^N \log \frac{\sum_{m=1}^M \exp(z_n^I \cdot z_m^T / \tau) \times \mathbb{1}(\hat{y}_n^I == m)}{\sum_{m=1}^M \exp(z_n^I \cdot z_m^T / \tau)}, \quad (8)$$

Table 1: Image recognition datasets used for open-vocabulary domain adaptation benchmark.

Dataset	Classes	Images	Domains	Description
Office [44]	31	4,110	4	Office objects from Amazon, DSLR, Webcam and Synthetic domains.
Office-home [57]	65	15,588	4	Office and Home objects from Art, Clipart, Product and Real-World domains.
Adaptiope [43]	123	36,900	3	Class-balanced object dataset with Product, Real-Life and Synthetic domains.
VisDA [40]	12	207,785	2	A large-scale common object dataset with synthetic and real domains.
ImageNet [7]	1,000	1,281,167	1	A large-scale real-world object dataset with a wide range of categories.
SUN397 [62]	397	76,129	1	A real-world indoor and outdoor scenes dataset for scene understanding.
Food101 [1]	101	75,750	1	A real-world food dish dataset for food recognition.
GTSRB [52]	43	26,640	1	A real-world german traffic sign dataset for sign recognition.
DTD [4]	47	3,760	1	A real-world describable texture image dataset for texture perception.
UCF101 [51]	101	9,537	1	A real-world human action video dataset for action recognition.

where z_n^I and z_m^T denote the encoded image and text features, i.e., $z_n^I = F^I(x_n^I)$ and $z_m^T = F^T(x_m^T)$. y_n^I stands for the pseudo label of x_n^I generated with δ_m^{IT} . The image-text prompt centroid δ_m^{IT} captures rich target image and text information. It is thus more invariant to visual and textual domain discrepancies and can “prompt” self-training to generate more accurate pseudo labels.

4 Experiments

4.1 Datasets

We benchmark our PEST extensively over 10 widely adopted image recognition datasets. As Table 1 shows, the 10 datasets have rich diversity, spanning multi-domain datasets with object images captured from several domains (e.g., real-world, synthetic, art, product and clipart domains) to single-domain datasets with real-world images for some specific visual task (e.g., the recognition of common objects, indoor and outdoor scenes, foods, traffic signs, natural textures and human actions).

Table 2: OVDA performance on multi-domain datasets of Office, Office-Home and Adaptiope.

ViT-B/16	Office					Office-Home					Adaptiope			
	A	W	D	S	Mean	A	C	P	R	Mean	P	R	S	Mean
CLIP [42]	77.9	79.4	76.9	56.7	72.7	74.4	58.5	79.6	79.4	72.9	82.6	78.2	45.9	68.9
ST [75]	78.6	81.1	78.3	68.6	76.6	77.8	62.5	81.3	80.3	75.4	86.7	82.0	49.5	72.7
CBST [76]	79.1	80.7	78.5	68.9	76.8	77.3	62.8	81.7	80.7	75.6	86.9	83.2	50.1	73.4
CRST [77]	78.8	81.2	79.1	69.0	77.0	78.1	63.1	81.4	81.1	75.9	87.1	83.9	50.7	73.9
SHOT [33]	79.2	81.1	81.2	67.1	77.1	77.9	64.3	80.9	81.5	76.1	88.3	84.7	51.2	74.7
MUST [31]	79.0	81.4	79.5	69.2	77.2	77.7	63.9	82.1	81.4	76.2	88.8	85.3	51.5	75.2
PEST (Ours)	84.3	82.8	81.3	72.3	80.1	78.9	68.9	85.7	82.4	78.9	91.8	88.1	59.8	79.9

ResNet-50	Office					Office-Home					Adaptiope			
	A	W	D	S	Mean	A	C	P	R	Mean	P	R	S	Mean
CLIP [42]	72.9	68.9	73.1	48.2	65.7	64.6	42.1	71.9	71.9	62.6	74.5	66.2	35.8	58.8
ST [75]	75.2	66.8	71.3	44.1	64.3	66.7	38.6	72.0	73.8	62.7	75.7	70.7	26.7	57.7
CBST [76]	75.2	67.8	72.2	51.1	66.5	68.1	41.5	73.6	74.5	64.4	77.2	71.1	34.3	60.8
CRST [77]	76.4	67.4	74.5	52.3	67.6	68.3	42.3	74.8	75.3	65.1	78.3	71.2	36.2	61.9
SHOT [33]	77.5	70.1	76.8	54.8	69.8	68.4	44.2	75.7	75.6	65.9	78.5	72.4	36.8	62.5
PEST (Ours)	79.6	75.3	80.3	55.0	72.5	68.6	47.9	78.2	77.4	68.0	80.7	75.6	37.8	64.7

ResNet-101	Office					Office-Home					Adaptiope			
	A	W	D	S	Mean	A	C	P	R	Mean	P	R	S	Mean
CLIP [42]	73.2	73.8	75.1	50.2	68.0	69.5	47.8	74.3	74.2	66.4	75.9	69.0	35.3	60.0
ST [75]	74.4	74.2	73.8	54.3	69.1	71.4	43.2	74.9	75.0	66.1	78.4	71.8	37.8	62.6
CBST [76]	74.6	75.9	72.9	58.1	70.3	72.3	44.9	77.7	76.2	67.7	79.5	73.3	41.5	64.7
CRST [77]	75.3	76.6	73.4	58.5	70.9	73.4	45.9	78.4	76.8	68.6	80.1	75.2	43.7	66.3
SHOT [33]	76.9	78.2	75.1	59.0	72.3	73.5	47.2	79.1	77.4	69.3	81.9	76.3	44.1	67.4
PEST (Ours)	80.1	81.2	77.5	61.9	75.1	74.6	51.2	82.6	78.9	71.8	85.3	78.8	45.7	69.9

4.2 Implementation Details

We conduct experiments with three popular backbones, i.e., ResNet-50 [17], ResNet-101 [17] and ViT-B [8] pre-trained by CLIP [42]. In training, we employ AdamW optimizer [36] with a weight decay of 0.05, and set the initial learning rate as $1e - 5$ which is adjusted with a cosine learning rate schedule. We use 2 GPUs with batch size 64 and the unsupervised adaptation training adds only a small amount of computation overhead after VLM pre-training. We set input image size as 224×224 and employ data augmentation policies of “RandomResizedCrop+Flip+RandAug” [5] to generate multiple image prompts. The momentum VLM image encoder is updated with a momentum coefficient of 0.99. All results except on ImageNet are obtained with above implementation details. For the large-scale ImageNet, we follow the implementations in [31] and use 16 GPUs with batch size 1024. During evaluation, we simply use the center-cropped image.

4.3 OVDA on Multi-domain Datasets

Tables 2-3 report the image classification results on 4 representative multi-domain datasets. The experiments were conducted with 3 representative backbones, i.e., ResNet-50, ResNet-101 and ViT-B/16. It can be seen that our PEST achieves superior performance consistently over various domains as compared with state-of-the-art methods. Besides, PEST outperforms CLIP substantially on Office (S)ynthetic domain, Office-Home (C)lipart domain and Adaptope (S)ynthetic domain with 15.6%, 10.4% and 13.9% accuracy improvement, respectively, showing that PEST can well handle the target domains with large domain discrepancies, i.e., Synthetic and Clipart styles.

Table 3: OVDA performance on large-scale multi-domain dataset VisDA.

VisDA Synthesis Domain													
ViT-B/16	plane	bcycl	bus	car	horse	knife	meycl	person	plant	sktbrd	train	truck	Per-class
CLIP [42]	98.5	99.7	64.6	92.5	99.7	96.8	85.3	98.4	99.8	79.4	66.4	73.4	87.8
ST [75]	97.2	99.9	60.4	84.5	99.8	98.6	92.5	99.7	99.9	79.3	74.2	84.4	89.2
CBST [76]	98.4	99.7	67.3	85.2	99.8	99.1	95.3	99.9	99.4	83.4	83.4	87.4	91.5
CRST [77]	98.1	98.2	70.5	86.5	98.6	98.7	94.3	98.8	97.8	86.7	88.7	86.1	91.9
SHOT [33]	99.6	99.1	74.6	86.3	98.3	99.3	96.4	96.1	99.7	87.5	90.1	87.3	92.2
MUST [31]	98.7	99.2	76.3	86.4	99.6	99.2	95.3	99.3	99.8	89.2	89.9	82.6	92.9
PEST (Ours)	99.7	99.7	78.9	86.6	99.9	99.3	96.4	99.4	99.8	91.9	90.8	93.2	94.6
VisDA Real Domain													
ViT-B/16	plane	bcycl	bus	car	horse	knife	meycl	person	plant	sktbrd	train	truck	Per-class
CLIP [42]	98.9	91.0	90.5	65.7	98.6	89.1	95.3	56.5	90.2	96.8	93.8	75.8	86.8
ST [75]	99.4	87.3	92.5	68.3	98.1	90.4	94.6	69.3	91.2	96.7	94.5	66.4	87.3
CBST [76]	99.3	89.2	91.3	76.9	98.2	89.5	95.4	68.1	88.4	96.4	94.1	64.2	87.5
CRST [77]	99.1	90.7	91.4	64.5	99.1	93.4	95.1	68.2	91.3	96.8	95.3	67.2	87.6
SHOT [33]	99.3	92.8	91.9	65.3	98.7	95.2	94.5	67.7	92.1	96.9	95.4	67.9	88.1
MUST [31]	99.2	95.7	92.6	56.9	99.1	98.6	96.0	67.0	93.5	98.8	96.9	68.1	88.5
PEST (Ours)	99.2	95.9	92.1	66.1	99.2	97.8	96.7	70.8	92.7	98.4	96.2	74.6	90.0

4.4 OVDA on Single-domain Datasets

Table 4 reports the image classification over 5 popular single-domain datasets. The experiments were conducted with 3 representative backbones, i.e., ResNet-50, ResNet-101 and ViT-B/16 (the results with ResNet-101 are provided in appendix B). We can observe that PEST outperforms the state-of-the-arts by large margins consistently over different task-specific datasets, demonstrating that it can effectively handle various new visual recognition tasks by using unlabelled data. In addition, PEST brings substantial improvements upon CLIP over SUN397 (e.g., +11.0% on ViT-B/16) and GTSRB (e.g., +16.8% on ViT-B/16), showing that PEST can well tackle new image classification tasks with very specific objectives, e.g., indoor/outdoor scene and German traffic sign recognition.

4.5 OVDA on General Dataset ImageNet

Table 5 presents the image classification results on ImageNet. It can be seen that PEST achieves superior performance as compared with state-of-the-art unsupervised methods, demonstrating the effectiveness of PEST over the very diverse and large-scale ImageNet. Besides, PEST surpasses 16-shot supervised methods by a clear margin (i.e., +7.2%), validating its advantages as a supervised

Table 4: OVDA performance on single-domain datasets of various image recognition tasks.

Method	ViT-B						ResNet-50					
	SUN397	Food101	GTSRB	DTD	UCF101	Mean	SUN397	Food101	GTSRB	DTD	UCF101	Mean
CLIP [42]	60.8	85.6	32.5	44.5	64.1	57.5	54.0	73.1	25.0	39.8	56.0	49.5
ST [75]	65.8	88.2	32.8	45.0	67.0	59.7	59.0	74.4	20.5	35.8	56.4	49.2
CBST [76]	63.2	89.5	37.6	44.3	68.1	60.5	63.7	78.2	27.4	38.7	59.5	53.5
CRST [77]	64.7	89.1	39.7	45.3	68.6	61.4	64.2	76.5	30.1	39.4	61.3	54.3
SHOT [33]	66.1	89.6	41.2	46.3	69.4	62.5	65.1	77.3	34.6	41.2	62.7	56.1
MUST [31]	67.7	89.4	42.7	46.5	70.6	63.3	-	-	-	-	-	-
PEST (Ours)	71.8	91.1	49.3	52.7	73.9	67.7	65.7	79.5	39.6	49.4	65.6	59.9

method to mitigate the image annotation constraint and facilitate deep network training while handling new visual recognition tasks.

Table 5: Comparison with few-shot supervised adaptation methods and unsupervised adaption methods on ImageNet. All methods use the same CLIP ViT-B/16 model.

Method	CLIP [42]	Supervised with 16 Labels per Class		Unsupervised		
		CoCoOp [73]	CoOp [74]	ST [75]	MUST [31]	PEST (Ours)
ImageNet Accuracy	68.3	71.0	71.5	76.5	77.7	78.7

4.6 Discussion

Generalization across different domains and tasks. We examine the generalization of PEST with respect to image recognition tasks and domains. Specifically, we perform extensive evaluations over 10 widely studied multi-domain [44, 57, 43, 40] and single-domain [7, 62, 1, 52, 4, 51] datasets as described in Table 1. Experimental results in Tables 2- 5 show that the proposed PEST achieves superior image recognition performance consistently across different domains and tasks.

Generalization across different backbones. We study the generalization of PEST by assessing it with three popular image recognition backbones, including two CNNs (i.e., ResNet-50 and ResNet-101) and one Transformer (i.e., ViT-B/16). Results in Tables 2- 5 and the tables in appendix B show that our PEST works effectively and consistently over different image recognition backbones.

Table 6: Ablation studies of PEST with ViT-B/16 on Office dataset.

Method	Vision-Language Prompt Ensemble		Temporal Prompt Ensemble	Office (Mean)
	Vision Prompt Ensemble	Language Prompt Ensemble		
CLIP [42]				72.7
ST [75]				76.6
	✓			77.5
		✓		78.2
	✓	✓		78.7
PEST	✓	✓	✓	80.1

Ablation study. We conduct ablation studies with ViT-B/16 on Office as shown in Table 6. As the core of the proposed PEST, we examine how our designed *vision prompt ensemble*, *language prompt ensemble* and *temporal prompt ensemble* contribute to the overall performance of open-vocabulary domain adaptation. As shown in Table 6, including either vision prompt ensemble or language prompt ensemble above self-training improves performance clearly, showing that image and text prompts ensembling help mitigate cross-domain discrepancies in image distributions and text distributions and can “prompt” unsupervised self-training with more accurate pseudo label prediction. In addition, combining vision and language prompt ensemble performs clearly better, indicating that the two types of prompt ensembling complement each other by working from orthogonal vision and language perspectives. Furthermore, including *temporal prompt ensemble* upon vision-language prompt ensemble (PEST in the last row) performs the best. It demonstrates the importance of temporal prompt ensemble that helps memorize previously learnt target information along the training process.

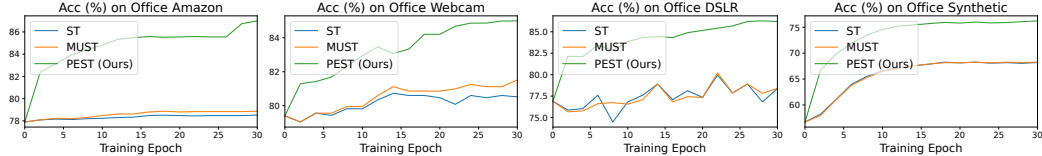


Figure 3: Pseudo label accuracy along the unsupervised adaptation process in OVDA (with ViT-B/16).

Parameter study. The parameter λ in Eq. 6 controls the update speed of temporal ensemble. We investigate λ by varying it from 0.9 to 0.9999 progressively, as shown in Table 7. It can be seen that varying λ does not affect OVDA clearly. The performance drops a bit while $\lambda = 0.9$, largely because a fast update may lead to unstable temporal prompt ensemble that only captures local information within each training batch.

Comparison with multi-prompt learning methods.

We compare PEST with multi-prompt learning strategies that explore complementary advantages of different prompts via uniform averaging [28, 49, 66], weighted averaging [28, 41, 49], majority voting [30, 14]. As Table 8 shows, existing multi-prompt learning methods do not perform well, largely because they were designed for NLP without considering the joint exploitation of vision and language modalities and the information memorization during unsupervised transfer. PEST instead learns and memorizes effective image-text correspondences in the unlabelled target domains via joint exploitation of vision and language information, which are essential to OVDA.

Pseudo label accuracy. Fig. 3 shows the pseudo label accuracy along the unsupervised adaptation process. PEST generates much more accurate pseudo labels than the vanilla self-training (ST) and the state-of-the-art MUST. The superior pseudo label accuracy is largely attributed to the proposed prompt ensemble which helps capture rich target image and text information that is more invariant to visual and textual domain discrepancies and can “prompt” better unsupervised self-training.

Comparison with MUST. MUST [31] tackles unsupervised adaptation of VLMs from the perspective of Masked Image Modelling [16] that heavily relies on Transformer backbones [8]. As a comparison, the proposed PEST works from the perspective of multiple-prompt learning that is independent to vision backbones. Thus, PEST can seamlessly work on different vision backbones like CNNs and Transformers as shown in Tables 2-4. In addition, Tables 2-5 show that PEST outperforms MUST clearly, largely because MUST exploits vision information largely while PEST exploits both vision and language information jointly which is better aligned with the objective of OVDA.

Prompt engineering. Both CLIP [42] and MUST [31] mitigate the cross-domain text distribution gap by prompt engineering [42] and ensembling, e.g., uniform averaging of 80 hand-crafted prompt templates on ImageNet. Although hand-crafted prompt templates bring clear gains, manually designing prompts for each new image recognition task and domain is laborious and time-consuming and degrades the scalability greatly. As Table 9 shows, without any prompt engineering, the proposed PEST still outperforms CLIP and MUST with clear margins, demonstrating its effectiveness and efficiency in handling new visual recognition tasks without prompt engineering. Note we did not include multi-domain datasets [44, 57, 43, 40] in this experiment due to the lack of hand-crafted prompt templates.

Due to the space limit, we provide more dataset details, experiments and discussions in the appendix.

Table 7: Parameter ablations with ViT-B/16 on Office. The default is marked in gray.

Parameter λ	0.9	0.99	0.999	0.9999
Office (Mean)	79.6	80.1	80.1	80.0

Table 8: Comparison with other multi-prompt learning methods with ViT-B/16 on Office.

Method	Office (Mean)
ST + Uniform Averaging [28]	77.2
ST + Weighted Averaging [41]	77.4
ST + Majority Voting [30]	77.1
PEST (Ours)	80.1

Table 9: Results of w/ and w/o prompt engineering with ViT-B/16 on 5 tasks of SUN397, Food101, GTSRB, DTD and UCF101.

Method	5-task Mean
CLIP w/o Prompt Engineering	57.5
CLIP w/ Prompt Engineering	62.0
MUST w/o Prompt Engineering	63.3
MUST w/ Prompt Engineering	65.8
PEST w/o Prompt Engineering	67.7

5 Conclusion

This paper presents PEST, a novel open-vocabulary domain adaptation framework that explores multi-prompt learning to learn effective image-text correspondences over unlabelled target images. PEST exploits prompt ensemble over vision, language and temporal dimensions for simultaneous mitigation of image and text discrepancies across domains. It requires merely a pre-trained VLM but achieves effective and efficient UDA towards arbitrary unlabelled target domains, demonstrating its superiority in facilitating deep network training while handling arbitrary new visual recognition tasks and domains. Extensive experiments show that PEST achieves superb recognition performance consistently across different backbones and image recognition tasks and domains. Moving forward, we will explore multi-prompt learning for other vision tasks such image generation.

References

- [1] Lukas Bossard, Matthieu Guillaumin, and Luc Van Gool. Food-101—mining discriminative components with random forests. In *Computer Vision—ECCV 2014: 13th European Conference, Zurich, Switzerland, September 6–12, 2014, Proceedings, Part VI 13*, pages 446–461. Springer, 2014.
- [2] Tom Brown, Benjamin Mann, Nick Ryder, Melanie Subbiah, Jared D Kaplan, Prafulla Dhariwal, Arvind Neelakantan, Pranav Shyam, Girish Sastry, Amanda Askell, et al. Language models are few-shot learners. *Advances in neural information processing systems*, 33:1877–1901, 2020.
- [3] Yuhua Chen, Wen Li, and Luc Van Gool. Road: Reality oriented adaptation for semantic segmentation of urban scenes. In *Proceedings of the IEEE Conference on Computer Vision and Pattern Recognition*, pages 7892–7901, 2018.
- [4] Mircea Cimpoi, Subhansu Maji, Iasonas Kokkinos, Sammy Mohamed, and Andrea Vedaldi. Describing textures in the wild. In *Proceedings of the IEEE conference on computer vision and pattern recognition*, pages 3606–3613, 2014.
- [5] Ekin D Cubuk, Barret Zoph, Jonathon Shlens, and Quoc V Le. Randaugment: Practical automated data augmentation with a reduced search space. In *Proceedings of the IEEE/CVF conference on computer vision and pattern recognition workshops*, pages 702–703, 2020.
- [6] Leyang Cui, Yu Wu, Jian Liu, Sen Yang, and Yue Zhang. Template-based named entity recognition using bart. *arXiv preprint arXiv:2106.01760*, 2021.
- [7] Jia Deng, Wei Dong, Richard Socher, Li-Jia Li, Kai Li, and Li Fei-Fei. Imagenet: A large-scale hierarchical image database. In *2009 IEEE conference on computer vision and pattern recognition*, pages 248–255. Ieee, 2009.
- [8] Alexey Dosovitskiy, Lucas Beyer, Alexander Kolesnikov, Dirk Weissenborn, Xiaohua Zhai, Thomas Unterthiner, Mostafa Dehghani, Matthias Minderer, Georg Heigold, Sylvain Gelly, et al. An image is worth 16x16 words: Transformers for image recognition at scale. *arXiv preprint arXiv:2010.11929*, 2020.
- [9] Tianyu Gao, Adam Fisch, and Danqi Chen. Making pre-trained language models better few-shot learners. *arXiv preprint arXiv:2012.15723*, 2020.
- [10] Dayan Guan, Jiaying Huang, Shijian Lu, and Aoran Xiao. Scale variance minimization for unsupervised domain adaptation in image segmentation. *Pattern Recognition*, 112:107764, 2021.
- [11] Dayan Guan, Jiaying Huang, Aoran Xiao, and Shijian Lu. Domain adaptive video segmentation via temporal consistency regularization. In *Proceedings of the IEEE/CVF International Conference on Computer Vision*, pages 8053–8064, 2021.
- [12] Dayan Guan, Jiaying Huang, Aoran Xiao, Shijian Lu, and Yanpeng Cao. Uncertainty-aware unsupervised domain adaptation in object detection. *IEEE Transactions on Multimedia*, 2021.
- [13] Kelvin Guu, Tatsunori B Hashimoto, Yonatan Oren, and Percy Liang. Generating sentences by editing prototypes. *Transactions of the Association for Computational Linguistics*, 6:437–450, 2018.
- [14] Karen Hambardzumyan, Hrant Khachatrian, and Jonathan May. Warp: Word-level adversarial reprogramming. *arXiv preprint arXiv:2101.00121*, 2021.
- [15] Xu Han, Weilin Zhao, Ning Ding, Zhiyuan Liu, and Maosong Sun. Ptr: Prompt tuning with rules for text classification. *AI Open*, 3:182–192, 2022.
- [16] Kaiming He, Xinlei Chen, Saining Xie, Yanghao Li, Piotr Dollár, and Ross Girshick. Masked autoencoders are scalable vision learners. *arXiv preprint arXiv:2111.06377*, 2021.
- [17] Kaiming He, Xiangyu Zhang, Shaoqing Ren, and Jian Sun. Deep residual learning for image recognition. In *Proceedings of the IEEE conference on computer vision and pattern recognition*, pages 770–778, 2016.

- [18] Judy Hoffman, Eric Tzeng, Taesung Park, Jun-Yan Zhu, Phillip Isola, Kate Saenko, Alexei Efros, and Trevor Darrell. Cycada: Cycle-consistent adversarial domain adaptation. In *International Conference on Machine Learning*, pages 1989–1998, 2018.
- [19] Weixiang Hong, Zhenzhen Wang, Ming Yang, and Junsong Yuan. Conditional generative adversarial network for structured domain adaptation. In *Proceedings of the IEEE Conference on Computer Vision and Pattern Recognition*, pages 1335–1344, 2018.
- [20] Jiaxing Huang, Dayan Guan, Shijian Lu, and Aoran Xiao. Mlan: Multi-level adversarial network for domain adaptive semantic segmentation. *Pattern Recognition*, 2021.
- [21] Jiaxing Huang, Dayan Guan, Aoran Xiao, and Shijian Lu. Category contrast for unsupervised domain adaptation in visual tasks. *arXiv preprint arXiv:2106.02885*, 2021.
- [22] Jiaxing Huang, Dayan Guan, Aoran Xiao, and Shijian Lu. Cross-view regularization for domain adaptive panoptic segmentation. In *Proceedings of the IEEE/CVF Conference on Computer Vision and Pattern Recognition*, pages 10133–10144, 2021.
- [23] Jiaxing Huang, Dayan Guan, Aoran Xiao, and Shijian Lu. Fsd: Frequency space domain randomization for domain generalization. In *Proceedings of the IEEE/CVF Conference on Computer Vision and Pattern Recognition*, pages 6891–6902, 2021.
- [24] Jiaxing Huang, Dayan Guan, Aoran Xiao, and Shijian Lu. Model adaptation: Historical contrastive learning for unsupervised domain adaptation without source data. *Advances in Neural Information Processing Systems*, 34:3635–3649, 2021.
- [25] Jiaxing Huang, Dayan Guan, Aoran Xiao, and Shijian Lu. Rda: Robust domain adaptation via fourier adversarial attacking. In *Proceedings of the IEEE/CVF International Conference on Computer Vision (ICCV)*, 2021.
- [26] Jiaxing Huang, Shijian Lu, Dayan Guan, and Xiaobing Zhang. Contextual-relation consistent domain adaptation for semantic segmentation. In *European Conference on Computer Vision*, pages 705–722. Springer, 2020.
- [27] Chao Jia, Yinfei Yang, Ye Xia, Yi-Ting Chen, Zarana Parekh, Hieu Pham, Quoc Le, Yun-Hsuan Sung, Zhen Li, and Tom Duerig. Scaling up visual and vision-language representation learning with noisy text supervision. In *International Conference on Machine Learning*, pages 4904–4916. PMLR, 2021.
- [28] Zhengbao Jiang, Frank F Xu, Jun Araki, and Graham Neubig. How can we know what language models know? *Transactions of the Association for Computational Linguistics*, 8:423–438, 2020.
- [29] Sawan Kumar and Partha Talukdar. Reordering examples helps during priming-based few-shot learning. *arXiv preprint arXiv:2106.01751*, 2021.
- [30] Brian Lester, Rami Al-Rfou, and Noah Constant. The power of scale for parameter-efficient prompt tuning. *arXiv preprint arXiv:2104.08691*, 2021.
- [31] Junnan Li, Silvio Savarese, and Steven CH Hoi. Masked unsupervised self-training for zero-shot image classification. *arXiv preprint arXiv:2206.02967*, 2022.
- [32] Yunsheng Li, Lu Yuan, and Nuno Vasconcelos. Bidirectional learning for domain adaptation of semantic segmentation. In *Proceedings of the IEEE Conference on Computer Vision and Pattern Recognition*, pages 6936–6945, 2019.
- [33] Jian Liang, Dapeng Hu, and Jiashi Feng. Do we really need to access the source data? source hypothesis transfer for unsupervised domain adaptation. In *International Conference on Machine Learning*, pages 6028–6039. PMLR, 2020.
- [34] Jian Liang, Dapeng Hu, Yunbo Wang, Ran He, and Jiashi Feng. Source data-absent unsupervised domain adaptation through hypothesis transfer and labeling transfer. *IEEE Transactions on Pattern Analysis and Machine Intelligence*, 2021.
- [35] Jiachang Liu, Dinghan Shen, Yizhe Zhang, Bill Dolan, Lawrence Carin, and Weizhu Chen. What makes good in-context examples for gpt-3? *arXiv preprint arXiv:2101.06804*, 2021.
- [36] Ilya Loshchilov and Frank Hutter. Decoupled weight decay regularization. *arXiv preprint arXiv:1711.05101*, 2017.
- [37] Yao Lu, Max Bartolo, Alastair Moore, Sebastian Riedel, and Pontus Stenetorp. Fantastically ordered prompts and where to find them: Overcoming few-shot prompt order sensitivity. *arXiv preprint arXiv:2104.08786*, 2021.
- [38] Timo Lüddecke and Alexander Ecker. Image segmentation using text and image prompts. In *Proceedings of the IEEE/CVF Conference on Computer Vision and Pattern Recognition*, pages 7086–7096, 2022.
- [39] Yawei Luo, Liang Zheng, Tao Guan, Junqing Yu, and Yi Yang. Taking a closer look at domain shift: Category-level adversaries for semantics consistent domain adaptation. In *Proceedings of the IEEE Conference on Computer Vision and Pattern Recognition*, pages 2507–2516, 2019.

- [40] Xingchao Peng, Ben Usman, Neela Kaushik, Judy Hoffman, Dequan Wang, and Kate Saenko. Visda: The visual domain adaptation challenge. *arXiv preprint arXiv:1710.06924*, 2017.
- [41] Guanghui Qin and Jason Eisner. Learning how to ask: Querying lms with mixtures of soft prompts. *arXiv preprint arXiv:2104.06599*, 2021.
- [42] Alec Radford, Jong Wook Kim, Chris Hallacy, Aditya Ramesh, Gabriel Goh, Sandhini Agarwal, Girish Sastry, Amanda Askell, Pamela Mishkin, Jack Clark, et al. Learning transferable visual models from natural language supervision. In *International Conference on Machine Learning*, pages 8748–8763. PMLR, 2021.
- [43] Tobias Ringwald and Rainer Stiefelhagen. Adaptope: A modern benchmark for unsupervised domain adaptation. In *Proceedings of the IEEE/CVF Winter Conference on Applications of Computer Vision*, pages 101–110, 2021.
- [44] Kate Saenko, Brian Kulis, Mario Fritz, and Trevor Darrell. Adapting visual category models to new domains. In *ECCV*, 2010.
- [45] Kuniaki Saito, Yoshitaka Ushiku, Tatsuya Harada, and Kate Saenko. Adversarial dropout regularization. *arXiv preprint arXiv:1711.01575*, 2017.
- [46] Kuniaki Saito, Kohei Watanabe, Yoshitaka Ushiku, and Tatsuya Harada. Maximum classifier discrepancy for unsupervised domain adaptation. In *Proceedings of the IEEE Conference on Computer Vision and Pattern Recognition*, pages 3723–3732, 2018.
- [47] Fatemeh Sadat Saleh, Mohammad Sadegh Aliakbarian, Mathieu Salzmann, Lars Petersson, and Jose M Alvarez. Effective use of synthetic data for urban scene semantic segmentation. In *European Conference on Computer Vision*, pages 86–103. Springer, 2018.
- [48] Swami Sankaranarayanan, Yogesh Balaji, Arpit Jain, Ser Nam Lim, and Rama Chellappa. Learning from synthetic data: Addressing domain shift for semantic segmentation. In *Proceedings of the IEEE Conference on Computer Vision and Pattern Recognition*, pages 3752–3761, 2018.
- [49] Timo Schick and Hinrich Schütze. Exploiting cloze questions for few shot text classification and natural language inference. *arXiv preprint arXiv:2001.07676*, 2020.
- [50] Christoph Schuhmann, Richard Vencu, Romain Beaumont, Robert Kaczmarczyk, Clayton Mullis, Aarush Katta, Theo Coombes, Jenia Jitsev, and Aran Komatsuzaki. Laion-400m: Open dataset of clip-filtered 400 million image-text pairs. *arXiv preprint arXiv:2111.02114*, 2021.
- [51] Khuram Soomro, Amir Roshan Zamir, and Mubarak Shah. Ucf101: A dataset of 101 human actions classes from videos in the wild. *arXiv preprint arXiv:1212.0402*, 2012.
- [52] Johannes Stalkamp, Marc Schliepsing, Jan Salmen, and Christian Igel. The german traffic sign recognition benchmark: a multi-class classification competition. In *The 2011 international joint conference on neural networks*, pages 1453–1460. IEEE, 2011.
- [53] Yi-Hsuan Tsai, Wei-Chih Hung, Samuel Schulter, Kihyuk Sohn, Ming-Hsuan Yang, and Manmohan Chandraker. Learning to adapt structured output space for semantic segmentation. In *Proceedings of the IEEE Conference on Computer Vision and Pattern Recognition*, pages 7472–7481, 2018.
- [54] Yi-Hsuan Tsai, Kihyuk Sohn, Samuel Schulter, and Manmohan Chandraker. Domain adaptation for structured output via discriminative patch representations. In *Proceedings of the IEEE International Conference on Computer Vision*, pages 1456–1465, 2019.
- [55] Michael Tschannen, Basil Mustafa, and Neil Houlsby. Image-and-language understanding from pixels only. *arXiv preprint arXiv:2212.08045*, 2022.
- [56] Eric Tzeng, Judy Hoffman, Kate Saenko, and Trevor Darrell. Adversarial discriminative domain adaptation. In *Proceedings of the IEEE Conference on Computer Vision and Pattern Recognition*, pages 7167–7176, 2017.
- [57] Hemanth Venkateswara, Jose Eusebio, Shayok Chakraborty, and Sethuraman Panchanathan. Deep hashing network for unsupervised domain adaptation. In *CVPR*, 2017.
- [58] Tuan-Hung Vu, Himalaya Jain, Maxime Bucher, Matthieu Cord, and Patrick Pérez. Advent: Adversarial entropy minimization for domain adaptation in semantic segmentation. In *Proceedings of the IEEE Conference on Computer Vision and Pattern Recognition*, pages 2517–2526, 2019.
- [59] Ben Wang and Aran Komatsuzaki. Gpt-j-6b: A 6 billion parameter autoregressive language model. 2021.
- [60] Guoqiang Wei, Cuiling Lan, Wenjun Zeng, Zhizheng Zhang, and Zhibo Chen. Toalign: Task-oriented alignment for unsupervised domain adaptation. *35th Advances in Neural Information Processing Systems*, 2021.
- [61] Zhirong Wu, Yuanjun Xiong, Stella X Yu, and Dahua Lin. Unsupervised feature learning via non-parametric instance discrimination. In *Proceedings of the IEEE Conference on Computer Vision and Pattern Recognition*, pages 3733–3742, 2018.

- [62] Jianxiong Xiao, James Hays, Krista A Ehinger, Aude Oliva, and Antonio Torralba. Sun database: Large-scale scene recognition from abbey to zoo. In *2010 IEEE computer society conference on computer vision and pattern recognition*, pages 3485–3492. IEEE, 2010.
- [63] Yanchao Yang and Stefano Soatto. Fda: Fourier domain adaptation for semantic segmentation. In *Proceedings of the IEEE/CVF Conference on Computer Vision and Pattern Recognition*, pages 4085–4095, 2020.
- [64] Jiahui Yu, Zirui Wang, Vijay Vasudevan, Legg Yeung, Mojtaba Seyedhosseini, and Yonghui Wu. Coca: Contrastive captioners are image-text foundation models. *arXiv preprint arXiv:2205.01917*, 2022.
- [65] Lu Yuan, Dongdong Chen, Yi-Ling Chen, Noel Codella, Xiyang Dai, Jianfeng Gao, Houdong Hu, Xuedong Huang, Boxin Li, Chunyuan Li, et al. Florence: A new foundation model for computer vision. *arXiv preprint arXiv:2111.11432*, 2021.
- [66] Weizhe Yuan, Graham Neubig, and Pengfei Liu. Bartscore: Evaluating generated text as text generation. *Advances in Neural Information Processing Systems*, 34:27263–27277, 2021.
- [67] Yuhang Zang, Wei Li, Kaiyang Zhou, Chen Huang, and Chen Change Loy. Open-vocabulary detr with conditional matching. In *Computer Vision–ECCV 2022: 17th European Conference, Tel Aviv, Israel, October 23–27, 2022, Proceedings, Part IX*, pages 106–122. Springer, 2022.
- [68] Jingyi Zhang, Jiaying Huang, Sheng Jin, and Shijian Lu. Vision-language models for vision tasks: A survey. *arXiv preprint arXiv:2304.00685*, 2023.
- [69] Jingyi Zhang, Jiaying Huang, and Shijian Lu. Spectral unsupervised domain adaptation for visual recognition. *arXiv preprint arXiv:2106.06112*, 2021.
- [70] Jingyi Zhang, Jiaying Huang, Zhipeng Luo, Gongjie Zhang, and Shijian Lu. Da-detr: Domain adaptive detection transformer by hybrid attention. *arXiv preprint arXiv:2103.17084*, 2021.
- [71] Yang Zhang, Philip David, and Boqing Gong. Curriculum domain adaptation for semantic segmentation of urban scenes. In *Proceedings of the IEEE International Conference on Computer Vision*, pages 2020–2030, 2017.
- [72] Zhun Zhong, Liang Zheng, Zhiming Luo, Shaozi Li, and Yi Yang. Invariance matters: Exemplar memory for domain adaptive person re-identification. In *Proceedings of the IEEE Conference on Computer Vision and Pattern Recognition*, pages 598–607, 2019.
- [73] Kaiyang Zhou, Jingkang Yang, Chen Change Loy, and Ziwei Liu. Conditional prompt learning for vision-language models. In *Proceedings of the IEEE/CVF Conference on Computer Vision and Pattern Recognition*, pages 16816–16825, 2022.
- [74] Kaiyang Zhou, Jingkang Yang, Chen Change Loy, and Ziwei Liu. Learning to prompt for vision-language models. *International Journal of Computer Vision*, 130(9):2337–2348, 2022.
- [75] Xiaojin Jerry Zhu. Semi-supervised learning literature survey. 2005.
- [76] Yang Zou, Zhiding Yu, BVK Kumar, and Jinsong Wang. Unsupervised domain adaptation for semantic segmentation via class-balanced self-training. In *Proceedings of the European conference on computer vision (ECCV)*, pages 289–305, 2018.
- [77] Yang Zou, Zhiding Yu, Xiaofeng Liu, BVK Kumar, and Jinsong Wang. Confidence regularized self-training. In *Proceedings of the IEEE/CVF International Conference on Computer Vision*, pages 5982–5991, 2019.